Selection of Optimal Recording Sites in Electrocardiography and Magnetocardiography

Jazbinšek V.[1], Burghoff M.[2], Kosch O.[2], Steinhoff U.[2], Hren R.[1], Trahms L.[2], Trontelj Z.[1]

[1]Institute of Mathematics, Physics and Mechanics, University of Ljubljana, Ljubljana, Slovenia;
[2]Physikalisch-Technische Bundesanstalt, Berlin, Germany.

Introduction

In multichannel recordings of both electrocardiographic and magnetocardiographic signals we typically encounter the problem of redundancy and uniqueness of signal information contained in a large number of leads. To solve this problem, Lux et al. [1] in their seminal work developed a practical method of reducing electrocardiographic leads and applied it to the design of the 32-lead system. This widely-used and convenient system for recording body surface potential maps (BSPMs) has proven its clinical value in detecting focal or regional inhomogeneities of ventricular depolarization and repolarization properties (see [2,3] and references therein). Magnetic field maps (MFMs), constructed from multiple recordings of magnetic field above the anterior chest, also offer information about the regional cardiac events and complement that of BSPMs (see [4] and references therein). However, lead configuration of multichannel systems for recording MFMs was largely determined by the technological constraints. This approach left magnetocardiographic signals unexamined regarding their redundancy.

In this paper, we apply the technique developed by Lux [1] to select a limited array of magnetic field recording sites and to estimate from these sites total MFMs. To validate our methodology, we also used concurrently recorded BSPMs.

Methods

Algorithm. To reduce the number of recording sites, we followed the statistical estimation technique [1], where the magnetic field or electric potential at unmeasured sites $\boldsymbol{x}^{\mathrm{e}}$ are estimated from their values at measured sites $\boldsymbol{x}^{\mathrm{m}}$ by a linear transformation $\boldsymbol{T}$ such that

$$\boldsymbol{x}^{\mathrm{e}} = \boldsymbol{T}\boldsymbol{x}^{\mathrm{m}} = \boldsymbol{K}_{\mathrm{um}}\boldsymbol{K}_{\mathrm{mm}}^{-1}\boldsymbol{x}^{\mathrm{m}}, \qquad (1)$$

where $\boldsymbol{K}_{\mathrm{mm}}$ is a covariance matrix of the measured potential/field and $\boldsymbol{K}_{\mathrm{um}}$ is a cross covariance matrix between the measured and unmeasured potential/field. This estimator minimizes the root mean square error (RMS). An optimal subset of recording sites was found by sequential algorithm [1]; the recording site that had the highest correlated power ("information content") with all other sites was selected at each step.

Data acquisition. The database for this study consisted of BSPMs and MFMs obtained from 4 subjects with no known cardiac diseases. A protocol is explained in details elsewhere [5]. Briefly, MFMs over a large area with diameter of 37 cm near the front and the back thorax were obtained with a dense 119 B_z channels (Fig. 1) with a sampling rate of 1 kHz. In addition, 148 lead BSPMs were recorded. We used various combinations of these data sets as learning ($\boldsymbol{x}^{\mathrm{m}}$) and test ($\boldsymbol{y}^{\mathrm{m}}$) sets. The noise level, estimated from measured data in the region before P onset, was 200 fT and 10 μV for the MFMs and BSPMs, respectively.

Evaluation criteria. We evaluated the quality of estimated quantities $\boldsymbol{y}^{\mathrm{e}}$ from Eq. (1) by comparing them with the measured values $\boldsymbol{y}^{\mathrm{m}}$. We used various criteria, like RMS error and maximum (MAX) error, relative difference (RD) and correlation coefficient (CC), which are for the map at time t_j and N_u unmeasured sites defined as

$$\mathrm{RMS}(t_j) = \sqrt{\sum_{i=1}^{N_u}\left(y_{i,j}^{e} - y_{i,j}^{m}\right)^2 \Big/ N_u}\,, \qquad (2)$$

$$\mathrm{MAX}(t_j) = \max\left|y_{i,j}^{e} - y_{i,j}^{m}\right|_{i=1}^{N_u}, \qquad (3)$$

$$\mathrm{RD}(t_j) = 100\sqrt{\sum_{i=1}^{N_u}\left(y_{i,j}^{e} - y_{i,j}^{m}\right)^2 \Big/ \sum_{i=1}^{N_u}\left(y_{i,j}^{m}\right)^2}\,, \qquad (4)$$

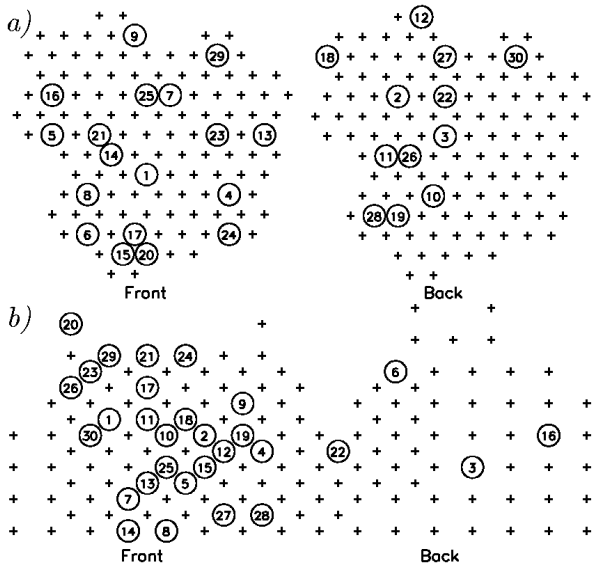

Fig. 1 Example of optimally selected recording sites when using measured data of three volunteers as a training set: a) 238 anterior/posterior MFM and b) 148-lead BSPM. Encircled numbers show the order of selected sites.

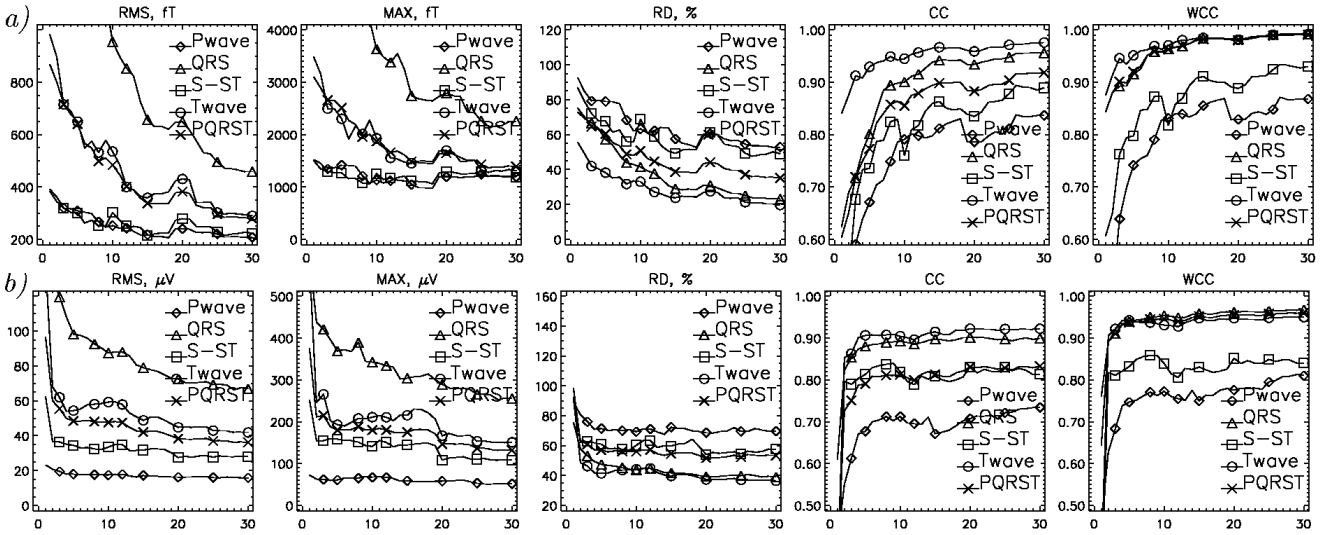

Fig. 2 Mean RMS, MAX, RD, CC and WCC vs. number of selected sites for a) MFMs and b) BSPMs when using all four combinations of learning ($\boldsymbol{x}^m$) and test ($\boldsymbol{y}^m$) data sets in cases where measurements on three of the four volunteers are used as $\boldsymbol{x}^m$ and measurements on the remaining volunteer are used as $\boldsymbol{y}^m$. After each selected site, maps ($\boldsymbol{y}^e$) for the $\boldsymbol{y}^m$ are estimated from Eq. (1) and for each $\boldsymbol{y}^e$, values of RMS, MAX, RD and CC are calculated from Eqs. (2-5). These results are then averaged over all maps on different time intervals, Pwave(◊), QRS(Δ), S–ST(□), Twave(○) and PQRST(×), and WCC is calculated from Eq. (6). Pwave interval is from the onset to the end of P, S–ST is a first 3/8 portion of the ST segment and Twave is from the end of S–ST to the end of T.

$$\mathrm{CC}(t_j) = \sum_{i=1}^{N_u} y^e_{i,j} y^m_{i,j} \Big/ \sqrt{\sum_{i=1}^{N_u} \left(y^e_{i,j}\right)^2 \left(y^m_{i,j}\right)^2} \,. \qquad (5)$$

To evaluate the similarity between the estimated and measured data set in different time intervals, like P-wave, QRS, S-ST, ST-T and PQRST, we calculated the mean values and standard deviations of the RMS, MAX, RD and CC values. In addition, we calculated the amplitude-weighted correlation coefficient (WCC) and the isointegral maps on those time intervals. The WCC on the time interval from t_1 to t_2 is defined as [6], $\mathrm{WCC} = \Sigma_{t_j=t_1}^{t_2} \mathrm{W}(t_j)\,\mathrm{CC}(t_j)$ where

$$\mathrm{W}(t_j) = \sum_{i=1}^{N_u} \left(y^m_{i,j}\right)^2 \Big/ \sum_{t_j=t_1}^{t_2} \sum_{i=1}^{N_u} \left(y^m_{i,j}\right)^2 \,. \qquad (6)$$

We defined the integral maps as an average over all maps on the selected time interval.

Results

Figure 1 shows the distribution of the first 30 selected recording sites for a case where a combination of data sets measured on three volunteers are used as a learning data set $\boldsymbol{x}^m$. The whole PQRST interval was used for $\boldsymbol{x}^m$, which included 500-700 map frames per volunteer. For the BSPM, most of sites are positioned on the anterior side of the thorax, while in the case of the MFM optimal recording sites are more evenly distributed over front and back.

Figure 2 shows average RMS, MAX, RD, CC and WCC when the data sets measured on three volunteers are used as $\boldsymbol{x}^m$ and the data measured on the remaining volunteer is used as $\boldsymbol{y}^m$. Results show that most of the information is stored in the first 10 to 20 optimally chosen sites. There is little information gain by selecting more than 20 sites. Average RMS, MAX, RD, CC and WCC calculated from the maps with 20 selected sites, obtained at different time intervals, are in the range of 240-650 fT, 1200-2800 fT, 28-60 %, 0.79-0.97 and 0.83-0.98 for the MFMs, and 16-72 μV, 60-290 μV, 37-80 %, 0.71-0.92 and 0.78-0.96 for the BSPMs, respectively. The RMS and MAX errors are higher for the QRS time interval, which may be expected since those errors are related to the amplitude of the signal. Average CCs and WCCs, which reflect similarity of the signal shape, are worse for the S-ST and especially for the P wave intervals, where the signal to noise ratio is lower. The WCCs are higher because the effect of noise is reduced during periods when the signal is small. Average RDs, which are sensitive both to the amplitude and the shape, are better for the QRS and the T wave regions.

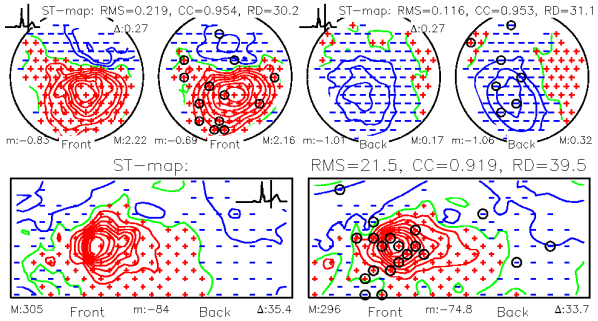

Fig. 3 Example of maps at the end of the S-ST interval after 20 selected channels from Fig. 1. Here m *and* M *are the minimal and the maximal map values and Δ is a step between the two isolines. All these values are in pT for the MFM and in μV for the BSPM. Positions of measured sites are shown by + and - in accordance with the sign of data. Estimated maps are displayed right to the corresponding measured maps. The selected sites are encircled, and RMS, CC and RD values are displayed above the estimated maps.*

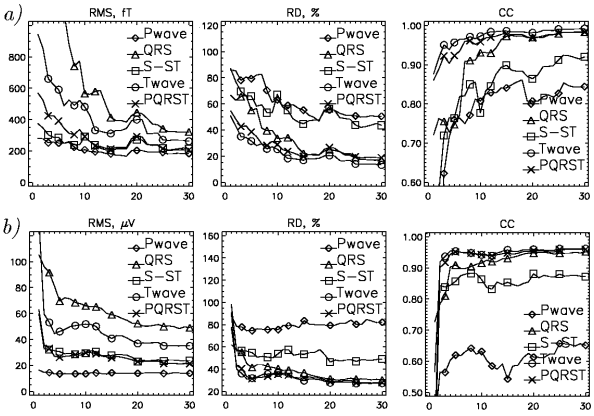

Fig. 4 Mean RMS, RD and CC vs. number of selected sites for a) MFM and b) BSPM integral maps, respectively, averaged over the same combinations of $\boldsymbol{x}^{m}$ *and* $\boldsymbol{y}^{m}$ *as in Fig. 2. We calculated from* $\boldsymbol{y}^{e}$ *integral maps on different time intervals (Pwave, QRS, S-ST, Twave,PQRST), and compared them with those obtained from* $\boldsymbol{y}^{m}$.

Figure 3 shows an example of measured and estimated MFM and BSPM when 20 sites are selected. Values of RMS, CC and RD are 219 fT, 0.954 and 30 % for the anterior MFM, 116 fT, 0.953 and 31 % for the posterior MFM, and 21.5 µV, 0.919 and 40 % for the BSPM, respectively.

Figure 4 shows the mean RMS errors, RDs and CCs when comparing integral maps calculated from measured and estimated data sets. Average values of those estimators for integral maps estimated from 12 selected sites are in the range of 190-580 fT, 18-58 % and 0.83-0.98 for MFMs, and 14-65 µV, 35-80 % and 0.58-0.94 for BSPMs, respectively. These ranges are comparable with those obtained for single maps estimated from 20 sites (see, Fig. 2, and description in the text). That may be expected since the procedure of averaging tends to reduce the information content.

Figure 5. shows an example of measured and estimated PQRST integral MFMs and BSPMs when 12 sites are selected. Values of RMS, CC and RD are 226 fT, 0.965 and 24 % for the anterior MFM, 99 fT, 0.981 and 22 % for the posterior MFM, and 18.1 µV, 0.96 and 30 % for the BSPM, respectively.

Discussion

This study is the first attempt to examine redundancy and uniqueness of MFM signal information. The main finding of our study is that markedly smaller number of leads, in comparison to that currently employed in systems for MFM recordings, may be sufficient to extract clinically pertinent information. We obtain the average WCC of 0.98±0.01 for estimated MFMs from 20 sites in the whole PQRST interval. This is evidently better then results in [6] (0.94±0.02 and 0.93±0.03), where the conversion between two MFM measuring system was evaluated by two methods, multipole expansion and minimum norm estimates.

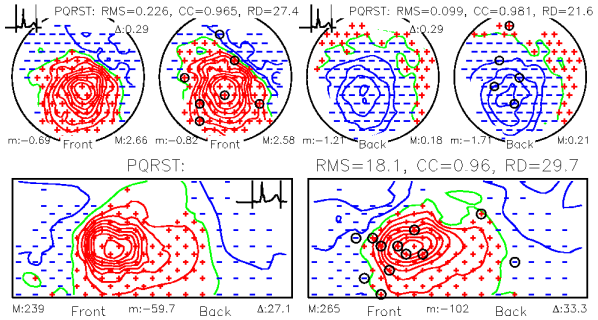

Fig. 5 PQRST – Integral maps after 12 optimally selected channels from Fig. 1, see also legend of Fig. 2.

Our results corroborate the finding in [1] that the "optimal" lead selection is non-unique, i.e., that slightly position of the first lead could generate quite different lead sets, which perform equally well. The database of our study consisted of healthy volunteers. The natural extension of this study could include patients with old myocardial infarction. The methodology developed in this study could also be used in selecting the optimal lead configuration for specific type of cardiac abnormalities, e.g., the limited array of magnetocardiographic leads for monitoring ST-segment changes caused by acute coronary ischemia.

References

[1] Lux RL, Smith CR, Wyatt RF, Abildskov JA. Limited lead selection for estimation of body surface potential maps in electrocardiography. IEEE Trans. Biomed. Eng., 1978, vol. 25: 270-276.

[2] Abildskov JA, Green LS. The recognition of arrhythmia vulnerability by body surface electrocardiographic mapping. Circulation, 1987, 75(Suppl III):79-83.

[3] Lux RL. Electrocardiographic mapping: Noninvasive electrophysiological cardiac imaging. Circulation, 1993, 87:1040-1042.

[4] Hren R, Steinhoff U, Gessner C, Endt P, Goedde P, Agrawal R, Oeff M, Lux RL, Trahms L. Value of magnetocardiographic QRST integral maps in the identification of patients at risk of ventricular arrhythmias. Pacing Clin. Electrophysiol., 1999, 22: 1292-1304.

[5] Jazbinsek V, Kosch O, Meindl P, Steinhoff U, Trontelj Z, Trahms L. Multichannel vector MFM and BSPM of chest and back. In: Nenonen J, Ilmoniemi RJ, Katila T, Eds., 12th Int. Conf. on Biomagnetism, Espoo, Helsinki Univ. of Technology, 2001.

[6] Burghoff M, Nenonen J, Trahms L, Katila T. Conversion of magnetocardiographic recordings between two different multichannel SQUID devices, IEEE Trans. Biomed. Eng., 2000, vol. 47: 869-875.

Acknowledgements

This work was partly supported by MSZS, Republic of Slovenia and by the German-Slovene Bilateral Program.